Hoogsteen-Paired Homopurine [R_P-PS]-DNA and Homopyrimidine RNA Strands Form a Thermally Stable Parallel Duplex

Piotr Guga, Magdalena Janicka, Anna Maciaszek, Beata Rębowska, and Genowefa Nowak
Polish Academy of Sciences, Centre of Molecular and Macromolecular Studies, Department of Bioorganic Chemistry, Łódź, Poland

ABSTRACT Homopurine deoxyribonucleoside phosphorothioates possessing all internucleotide linkages of R_P configuration form a duplex with an RNA or 2′-OMe-RNA strand with Hoogsteen complementarity. The duplexes formed with RNA templates are thermally stable at pH 5.3, while those formed with a 2′-OMe-RNA are stable at neutrality. Melting temperature and fluorescence quenching experiments indicate that the strands are parallel. Remarkably, these duplexes are thermally more stable than parallel Hoogsteen duplexes and antiparallel Watson-Crick duplexes formed by unmodified homopurine DNA molecules of the same sequence with corresponding RNA templates.

INTRODUCTION

Higher structural order in DNA and RNA is characterized by a substantial degree of polymorphism, which is governed by several factors such as base sequence, concentration, temperature, pH, buffer composition, ionic strength, and others. Different structures can be stabilized by favorable stacking interactions, solvation, and hydrogen-bonding schemes. While Watson-Crick (WC) is the normal hydrogen-bonding scheme in complementary oligonucleotide antiparallel-stranded duplexes (1), DNA and RNA strands also have the capacity to adopt parallel-stranded conformations in which the purine-pyrimidine stretches may also form part of triplexes (2,3) and tetraplexes (4,5). In principle, at neutral pH, parallel duplexes can be stabilized by Donohue (reverse WC) type A-T, G-C basepairing (6), or Hoogsteen (H) A-T basepairing, while in mildly acidic conditions, cytosine N3 is protonated (at 25°C, pK_a 4.3 and 4.6 were found for CMP and dCMP, respectively (7)), and Hoogsteen G-C^+ basepairs can also exist (8). However, acidic pH seems not to be necessary for the latter stabilization because thermodynamic, UV, and NMR studies have been reported, showing (7,9) that, in a Py/Pu/Py DNA parallel triplex, the cytosines involved in Hoogsteen basepairing remain protonated at pH 7–7.2.

There are few reports of parallel stretches in native DNA because every system in vivo uses the Watson-Crick-type anti-parallel duplex between complementary strands. Tchurikov and co-workers reported parallel duplex formation for specific functions in local regions of DNA (10–12). Such a parallel duplex has been also detected in *Escherichia coli* mRNA (13). To date, parallel structures have been mostly investigated in vitro. The x-ray structure of a self-paired parallel cytidylyl-3′,5′-adenosine dimer of CpA with the protonated C-C pair and the neutral A-A pair (with intercalated proflavine dye) was reported by Westhof and Sundaralingam in 1980 (14). X-ray fiber diffraction studies showed that the formation of the parallel duplexes (stabilized by Hoogsteen-type hydrogen bonds) can be promoted by steric blocking of one side of the adenine ring, i.e., the N(1) side, which is used in Watson-Crick and reverse Watson-Crick pairings (15). The parallel-stranded duplex model, in which the A-T pairings are reverse Watson-Crick, was early described by Pattabiraman (16) and further refined by IR (17) and NMR (18,19) spectroscopy. Molecular dynamics simulations showed that sequences containing similar number of d(A-T) and d(G-C) pairs (which are nonisomorphous) arranged in a reverse Watson-Crick structure are unstable, while stable structures were found when Hoogsteen pairing was assumed (20).

Certain types of Hoogsteen paired parallel-stranded duplexes can be good templates for association of WC paired DNA or RNA targets resulting in the formation of parallel triplexes, where the Hoogsteen and central strand are of the same spatial orientation and the WC strand is antiparallel, as shown later in Scheme 2, structure **VIII** or **IX**. This can be very useful for the development of antigene or antisense therapies, provided that the templates are thermally sufficiently stable. For unmodified oligonucleotides, the thermal stability of parallel duplexes is significantly lower compared to antiparallel Watson-Crick duplexes. More stable parallel structures are formed by constructs consisting of a purine chain

Submitted March 12, 2007, and accepted for publication June 27, 2007.

Address reprint requests to P. Guga, Tel.: 48-42-680-3248; E-mail: pguga@bio.cbmm.lodz.pl.

Abbreviations used: C^+, protonated cytidine nucleotide; CPG, controlled pore glass; MALDI-TOF, matrix-assisted laser desorption ionization-time of flight; PAGE, polyacrylamide gel electrophoresis; PS-oligos, phosphorothioate analogues of DNA; RP-HPLC, reversed phase-high performance liquid chromatography; T_a, association temperature, the temperature in a thermal association experiment at which 50% of given DNA molecules have formed a complex and the other 50% remain separated; T_m, melting temperature, the temperature in a thermal dissociation experiment at which 50% of given DNA molecules still form a complex and the other 50% are separated; r.t., room temperature. In compound labels: Descriptors [R_P-PS], [Mix-PS] indicate phosphorothioate analogues of DNA possessing all phosphorus atoms of R_P or random absolute configuration, respectively; a descriptor [PO] indicates a natural, nonmodified DNA molecule; and a suffix **M** indicates 2′-OMe-RNA strands.

Editor: Kathleen B. Hall.

0006-3495/07/11/3567/08 $2.00

doi: 10.1529/biophysj.107.108183

linked to a pyrimidine chain of inverted polarity by 3′–3′ or 5′–5′ internucleotide junctions (21,22).

One can assume that the factors reported as those stabilizing parallel triplexes in fact predominantly stabilize the Hoogsteen duplex. The relatively weak binding of the third strand to the underlying WC antiparallel duplex is partly due to charge repulsion between three aligned polyanionic strands. Therefore, triplexes are stabilized by introducing easily protonated basic groups, in particular amines (23) or guanidines (24), into the third strand.

Since natural oligodeoxyribonucleotides are easily degraded by nucleases, several modifications of the sugar-phosphate backbone have been developed (25–28). Among them phosphorothioate analogs of DNA (PS-oligos) appear to be very important because of the close similarity of their properties to natural DNA and their enhanced stability against nucleolytic degradation. However, PS-oligos prepared by routine chemical methods consist of a mixture of diastereomers (29,30). The oxathiaphospholane approach developed in this laboratory allows for preparation of PS-oligos with a predetermined sense of P-chirality (31,32) and has made possible a correlation of their stereochemistry with the thermal stability of antiparallel duplexes. It was found that, usually, PS-oligos and complementary DNA and RNA strands form WC duplexes that are less stable than regular nonmodified oligonucleotides (33,34). However, there was recently a report from this laboratory on the thermal stability of RNA/[R_P-PS]-DNA/RNA triplexes containing a stereo-defined homopurine DNA strand with all phosphorothioate linkages of R_P absolute configuration, where the Hoogsteen RNA and the central phosphorothioate DNA strands are of the same polarity (35). Remarkably, these triplexes are thermally more stable than complexes formed by unmodified homopurine DNA molecules of the same sequence. Analogous and even more stable triplex structures were formed with the participation of the 2′-OMe RNA derivatives. Interestingly, contrary to the melting of typical triplexes where the Hoogsteen strands dissociate at low temperature, followed by higher temperature dissociation of Watson-Crick duplexes, in the case of RNA/[R_P-PS]-DNA/RNA triplexes only one transition at relatively high temperature was observed on the corresponding melting curves (Supplementary Material, Fig. 1S), although some premelting process could be noticed in some instances. Also, for a triplex consisting of 5′-fluorescein-(2′-OMe)-CUCCUUUCUCUC-3′, [R_P-PS]-5′-$BHQ_{PS\text{-}Mix}$GAGGAAAGAGAG-3′ (BHQ is a dark quencher moiety; see below) and 3′-(2′-OMe)-CUCCUUUCUCUC-5′, fluorescence-quenching studies indicated that, in a melting experiment, the BHQ-labeled homopurine phosphorothioate strand and Hoogsteen-paired fluorescein-labeled RNA strand remained associated up to 60°C and dissociated at higher temperatures. In this article, we present evidence that homopurine [R_P-PS]-DNA and a homopyrimidine RNA or 2′-OMe-RNA strand complementary in the Hoogsteen sense form a thermally stable parallel duplex.

MATERIALS AND METHODS

Sodium chloride and Tris base (both of Aristar quality) were purchased from BDH Laboratory Supplies (Poole, UK). Magnesium chloride pro analysi was obtained from Merck (Darmstadt, Germany). For the titration of Tris base, hydrochloric acid (amino-acid analysis grade reagent, Applied Biosystems, Foster City, CA) was used. Sodium acetate buffer of 0.1 M concentration (pH 5.3) was obtained by dilution of concentrated sodium acetate buffer (3 M, pH 5.5) supplied by Applied Biosystems. All absorption measurements and UV monitored melting experiments were carried out in a 1 cm path-length cell with a CINTRA 40 spectrophotometer (GBC, Dandenong, Australia), equipped with a Peltier thermocell.

Chemical synthesis of oligonucleotides

The synthesis of P-stereo-defined [PS]-oligonucleotides was performed manually. The first nucleoside units were anchored to the solid support by a sarcosinyl linker (36). Appropriately protected deoxyguanosyl and deoxyadenosyl monomers possessing 3′-*O*-(2-thio-''spiro''-4,4-pentamethylene-1,3,2-oxathiaphospholane) moiety were synthesized and separated chromatographically into pure diastereomers. The protocol for the synthesis has been previously described (31,32).

The synthesis of unmodified DNA, [Mix-PS]-DNA, RNA, and 2′-OMe-RNA oligonucleotides was performed on ABI 380B DNA or ABI 394 DNA/RNA synthesizers (Applied Biosystems) at a 1 μmol scale using standard phosphoramidite DNA and RNA protocols.

The fluorescently-labeled 2′-OMe-RNA oligomers were synthesized using the standard phosphoramidite method. For the synthesis of the oligonucleotides carrying 6-carboxyfluorescein at the 3′-end or 5′-end, appropriate CPG-support or phosphoramidite reagents were used (CPG, Lincoln Park, NJ).

The stereo-defined oligomer [R_P-PS]-d(GAGGAAAGAGAG), for labeling at the 5′-end with a static ''BHQ-1'' quencher (the dye has broad strong absorbance centered at $\sim\lambda_{max} = 534$ nm) to form [R_P-PS]-BHQ_{PS}d(GAGGAAAGAGAG) (**1B**), was synthesized manually on the solid support (see above). After detritylation it was reacted with a ''BHQ-1'' phosphoramidite (4′-(2-nitro-4-toluyldiazo)-2′-methoxy-5′-methyl-azobenzene-4″-(*N*-ethyl)-*N*-ethyl-2-cyanoethyl-(*N*,*N*-diisopropyl)-phosphoramidite; Glen Research, Sterling, VA) in the presence of 1H-tetrazole, followed by sulfurization. Thus, the phosphorothioate linkage of random configuration was formed between the quencher and the 5′-dG residue.

All synthesized oligomers were purified by two-step RP-HPLC (DMT-on and DMT-off), and their purity was assessed by MALDI-TOF mass spectrometry (a Voyager-Elite instrument operating in the reflector mode with detection of negative ions; PerSeptive Biosystems, Framingham, MA) and polyacrylamide gel electrophoresis.

Sample preparation and melting profile recording

The concentration of oligomers was determined spectrophotometrically by UV absorbance at λ_{max} in water, using extinction coefficients calculated by the standard method (37). Samples were then lyophilized and redissolved in 10 mM Tris-HCl, 100 mM NaCl, 10 mM $MgCl_2$ buffer (pH 7.4 or 5.3), or 10 mM Tris-HCl, 100 mM NaCl, 2.4 mM $MgCl_2$ buffer (pH 5.3). Melting profiles were measured at a total oligonucleotide concentration of 4.0 μM with a temperature gradient of 0.2°C/min with a detector set at 254 nm. The T_m values were calculated using the first-order derivative method.

Measurements of fluorescence

Fluorescence measurements were made in 1-cm cuvettes using a fluorescence spectrophotometer Cary Eclipse (Varian Australia, Clayton, South Australia) with a thermostatting Peltier element accessory. Samples at concentrations of 200 nM, 1 μM, or 2 μM were dissolved in a buffer containing 10 mM Tris-HCl,

100 mM NaCl, 10 mM $MgCl_2$ (pH 7.4). Spectra were recorded in triplicate. The excitation and emission slits were set at 5 or 10 nm.

Measurements of circular dichroism

CD spectra were recorded on a CD6 dichrograph (Jobin-Yvon, Longjumeau, France) using 5-mm path-length cells. Spectra were smoothed with a five-point algorithm provided by the manufacturer of the dichrograph.

RESULTS AND DISCUSSION

Studies by CD spectroscopy

Observations indicating the formation of a unique structure were done by comparison of CD spectra recorded during the temperature-driven association (85°C → 15°C) of the [R_P-PS]-dA_{12} or [PO]-dA_{12} mixed with (2′-OMe)-U_{12} strands. For [PO]-dA_{12} strands mixed with (2′-OMe)-U_{12} at a 1:1 or 1:2 molar ratio, the association-related CD spectra (Fig. 1 *A* and Supplementary Material, Fig. 2S, respectively) changed from high temperature spectra characteristic for single strands (a broad positive band of low intensity centered at 272 nm, crossover points at 260 and 290 nm) to low temperature spectra typical for an A-form helix (a broad positive band of high intensity centered at 268 nm, crossover points at 254 and 295 nm). While the overall A-conformation for [R_P-PS]-DNA/RNA duplexes has been reported in the literature (38–42), a notably different pattern of changes was observed for [R_P-PS]-dA_{12} mixed with (2′-OMe)-U_{12} at a 1:2 molar ratio (Fig. 1 *B*). Although at low temperature the positive band was centered at 264 nm, between 78° and 71°C its left crossover point rapidly blue-shifted from 260 nm to 252 nm and geometry of consecutive bands (recorded below 71°C) was different compared to those recorded for a mixture of [PO]-dA_{12} and (2′-OMe)-U_{12}. It must be emphasized that the blue-shift, indicating the structurization, was completed within the 78–71°C range (spectra were recorded starting from 85°C with 7°C decrements). However, we were surprised to see that for the [R_P-PS]-dA_{12} mixed with (2′-OMe)-U_{12} at a 1:1 molar ratio, the low temperature positive bands are very narrow (cross points at 250 and 270 nm) and blue-shifted to 258 nm. Moreover, they are accompanied by a negative band of medium intensity at 280 nm, not present in any spectrum showed in panels *A* and *B* (Fig. 1 *C*). Again, the blue-shift of the 260 nm crossover point was virtually complete between 78 and 71°C. To the best of our knowledge, such CD spectra have not been reported in the literature. To get a deeper insight into this phenomenon, from all three sets of the CD data (Fig. 1, *A–C*) corresponding difference spectra (Fig. 2, *A–C*, respectively) were derived by numerical subtraction of the initial spectra (recorded at 85°C) from consecutive spectra recorded at lower temperatures. These difference spectra revealed important distinctions between the observed patterns. For [PO]-dA_{12}/(2′-OMe)-U_{12} at a 1:2 molar ratio (Fig. 2 *A*), upon cooling from 78°C down to 43°C, there is increasing intensity of the positive band at ~275 nm, followed (upon further cooling) by a shift of a crossover point from 260 nm to 250 nm and increasing intensity of the 260 nm band. For the mixture [R_P-PS]-dA_{12}/(2′-OMe)-U_{12} (1:1 molar ratio; Fig. 2 *C*), even at temperature above 70°C, there is a negative band at 275 nm and positive band at ~257 nm, and both bands get more intensive when the sample is cooled down. Notably, the crosspoints at 248 and 267 nm remain virtually unchanged across

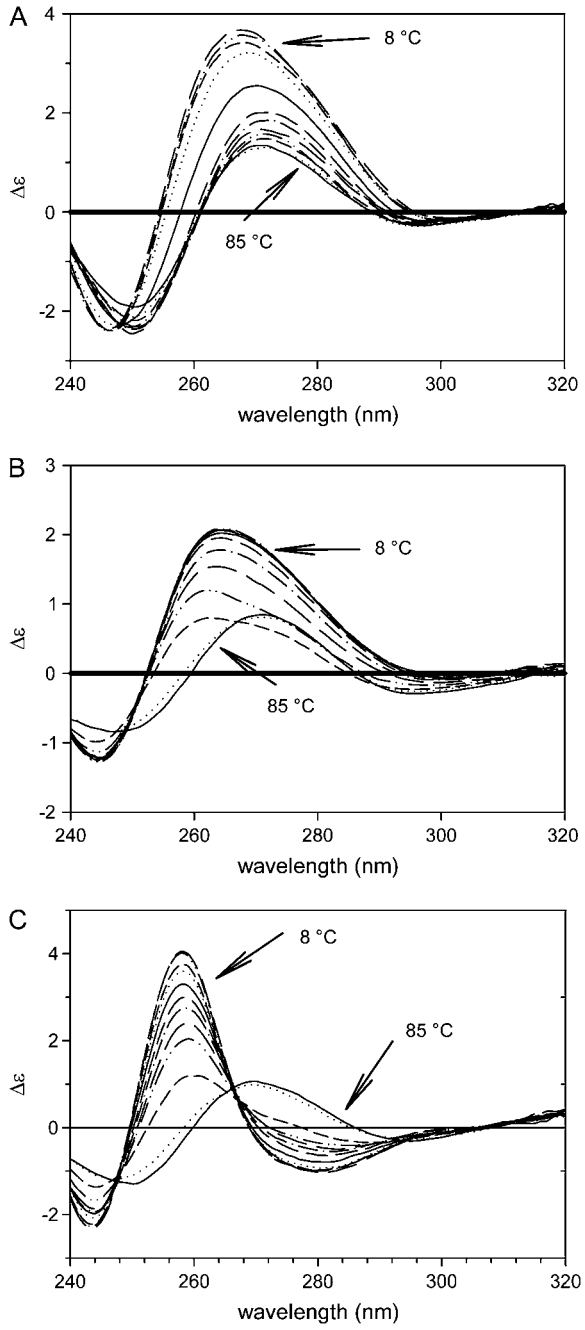

FIGURE 1 ORD CD spectra recorded during association experiment at given molar ratio of the DNA and RNA strands. (*A*) [PO]-dA_{12} + (2′-OMe)-U_{12}, (1:1); (*B*) [Rp-PS]-dA_{12} + (2′-OMe)-U_{12}, (1:2); and (*C*) [R_P-PS]-dA_{12} + (2′-OMe)-U_{12}, (1:1). Temperature 85°C → 8°C, with 7°C decrements.

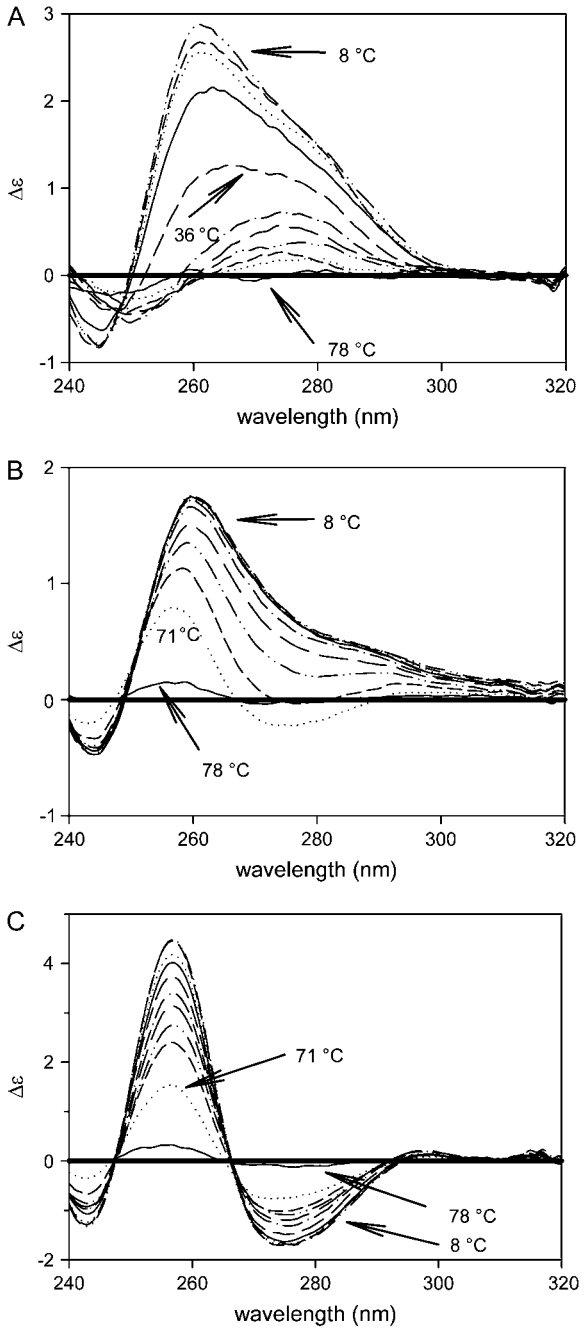

FIGURE 2 ORD CD difference spectra obtained numerically by subtraction of initial spectra recorded at 85°C from consecutive spectra recorded at lower temperatures. (*A*) [PO]-dA_{12} + (2′-OMe)-U_{12}, (1:1); (*B*) [R_P-PS]-dA_{12} + (2′-OMe)-U_{12}, (1:2); and (*C*) [Rp-PS]-dA_{12} + (2′-OMe)-U_{12}, (1:1). Temperature 85°C→8°C, with 7°C decrements.

the whole temperature range. This indicates that the basic structurization occurred at a very early stage of the association experiment and it cannot be attributed to the formation of a Watson-Crick duplex. For the mixture [R_P-PS]-dA_{12}/(2′-OMe)-U_{12} (1:2 molar ratio; Fig. 2 *B*), at temperature 71°C, there is a negative band at 275 nm and a positive band at ~257 nm. When the sample is cooled down, the latter band gets more intensive, while the negative band can be seen in all spectra as a concavity between 265 and 290 nm. Most likely, the concavity results from the superposition of the negative band on a positive band (of increasing intensity) at ~275 nm, which is observed for [PO]-dA_{12}/(2′-OMe)-U_{12} and is considered a strong indicator of the A-conformation. It should be noticed that the cross-point at 248 nm remains virtually unchanged.

Based on the dependence of the CD spectra on the PS-DNA:RNA stoichiometry we postulate that [R_P-PS]-dA_{12} and (2′-OMe)-U_{12} mixed at 1:1 ratio associate at high temperature (between 85 and 71°C) to form a parallel duplex. When both components are mixed at 1:2 ratio, in the curve recorded at 71°C a rapid shift of the positive band from 272 to 261 nm (Fig. 1 *B*) indicates virtually quantitative formation of a parallel duplex. As the temperature is further decreased, association of the excess U_{12} strand to the parallel duplex occurs in the Watson-Crick sense and this process is visualized by the growth of a ''shoulder'' between 268 and 280 nm and the decreasing concavity on the corresponding difference spectra. For the mixture of [PO]-dA_{12} and (2′-OMe)-U_{12} mixed at 1:1 ratio, structurization begins at a much lower temperature and neither the band at 272 nm nor its left crossover point move to shorter wavelengths down to 50°C (Fig. 1 *A*). Since at low temperatures the observed overall blue-shift of that band is small, the changes should be attributed to the formation of the anti-parallel duplex.

Polarity of strands—thermal stability studies

One can argue that symmetry or palindromicity of the A_{12} oligomer permits an alternative explanation, because the U_{12} molecules mixed even at 1:1 ratio, may simultaneously associate as Watson-Crick and Hoogsteen components. Therefore, to verify our hypothesis, nonpalindromic dodecameric sequences 5′-dGAGGAAAGAGAG-3′ (**1**), corresponding Hoogsteen-paired 5′-CUCCUUUCUCUC-3′ (**2**), and Watson-Crick paired 5′-CUCUCUUUCCUC-3′ (**3**) were selected for further experiments. The oligomer **1** is as nonpalindromic as possible to promote mismatch-free parallel association with **2** (structure **I**, Scheme 1) with discrimination of the competing Watson-Crick interactions (structures **II**–**V**, Scheme 1). For UV monitored thermal dissociation studies, three forms

Scheme 1. Structure **I** – a parallel duplex; structures **II**, **III**, **IV** and **V** – possible antiparallel duplexes with underlined mismatches.

2 5'-CUCCUUUCUCUC-3'
1 5'-GAGGAAAGAGAG-3'
I

1 5'- GAGGAAAGAGAG-3'
2 3'- CUCUCUUUCCUC-5'
III

1 5'-GAGGAAAGAGAG-3'
2 3'-CUCUCUUUCCUC-5'
V

1 5'- GAGGAAAGAGAG-3'
2 3'- CUCUCUUUCCUC-5'
II

1 5'- GAGGAAAGAGAG-3'
2 3'- CUCUCUUUCCUC-5'
IV

TABLE 1 Melting/association temperatures (°C) measured for complexes of different form of DNA strand 1 with RNA or 2′-OMe-RNA templates (equimolar mixtures) at neutral and acidic conditions

	pH 7.4, 10 mM $MgCl_2$					pH 5.3, 2′-OH-RNA template			
	2′-OMe-RNA			2′-OH-RNA*		2.4 mM $MgCl_2$		10 mM $MgCl_2$	
Form of DNA	WC **3M**	H **2M**	WC+H **3M**+**2M**	WC **3**	WC+H **3**+**2**	WC **3**	H **2**	WC **3**	H **2**
[PO]-**1**	43/43	−/−[†]	43/43	40/n.d.[‡]	40/40	35/35	34/29	40/40	35/33
[R_P-PS]-**1**	42/40	59/59	91/67	35/n.d.	60/37	40/37	51/36	44/43	50/42
[Mix-PS]-**1**	36/37	36/36	72/40	33/n.d	36/41	34/32	40/29	38/38	40/35

*No transition was observed for mixtures of any form of **1** with Hoogsteen-paired **2**.
[†]No transition observed.
[‡]*n.d.*, not determined.

of oligodeoxyribonucleotide **1** were synthesized, namely two phosphorothioate analogs with all phosphorus atoms of R_P configuration ([R_P-PS]-**1**) or random configuration ([Mix-PS]-**1**) and, as a reference compound, a nonmodified [PO]-**1**. In addition to the oligoribonucleotide sequences **2** and **3**, their 2′-OMe-analogs (**2M** and **3M**, respectively) were also synthesized. Melting curves were recorded at pH 7.4 or 5.3 in buffers containing 10 mM Tris-Cl, 100 mM NaCl and either 2.4 or 10 mM magnesium chloride (Table 1). No transition was observed on melting curves recorded for mixtures of any form of **1** with Hoogsteen-paired **2** (2′-OH-RNA) at neutral pH. When the WC-paired RNA strand **3** was added to the mixture [PO]-**1/2**, a T_m characteristic for the corresponding WC duplex was found (40°C). The formation of the WC duplex is further confirmed by a lack of hysteresis ($T_a = T_m$). In the case of [R_P-PS]-**1/2** mixed with **3**, a T_m of 60°C was measured and this (together with a 23°C hysteresis) indicates the formation of the triplex structure (35). However, when the 2′-OMe-RNA templates were used, the formation of a duplex (at neutrality; see Fig. 3) was observed for the mixtures [R_P-PS]-**1/2M** (*dotted line*) and [Mix-PS]-**1/2M** (*short dash line*) with $T_m = 59$°C and 36°C, respectively, with no hysteresis. Notably, there is no S-shape curve for the mixture [PO]-**1/2M** (*solid line*) that indicates low thermal stability of any complex. Upon addition of the WC-paired 2′-OMe-RNA strand **3M**, further increase of thermal stability of complexes **3M**/[R_P-PS]-**1/2M** (*long dash line*, $T_m = 91$°C) and **3M**/[Mix-PS]-**1/2M** (*dash-dot line*, $T_m = 72$°C) was observed, without any enhancement for **3M**/[PO]-**1/2M**.

Formation of thermally stable Hoogsteen duplexes by homopurine **1** mixed with 2′-OH-RNA template was enabled by acidic pH 5.3 (Fig. 4). Again, the most stable structures were [R_P-PS]-**1/2** ($T_m = 51$°C) and [Mix-PS]-**1/2** ($T_m = 40$°C). It should be pointed out that these duplexes were more stable than corresponding antiparallel duplexes formed with **2** ($T_m = 40$°C and 34°C, respectively), while the stability of [PO]-**1/2** ($T_m = 34$°C) was close to that of antiparallel [PO]-**1/3**. Raising the concentration of Mg^{+2} cations (10 mM vs. 2.4 mM) resulted in increased stability (by 4–5°C) of all three Watson-Crick duplexes (no hysteresis). The T_m values of Hoogsteen duplexes remained the same, although a 4–6°C increase of corresponding T_a values was

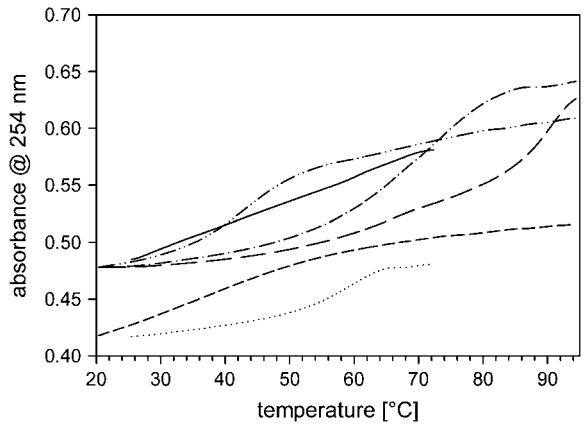

FIGURE 3 Melting curves recorded for [R_P-PS]-**1/2M** (*dotted line*, $T_m = 59$°C); [Mix-PS]-**1/2M** (*short dash line*, $T_m = 36$°C); [PO]-**1/2M** (*solid line*); **3M**/[R_P-PS]-**1/2M** (*long dash line*, $T_m = 91$°C); and **3M**/[Mix-PS]-**1/2M** (*dash-dot line*, $T_m = 72$°C). Buffer 10 mM Tris-HCl, 100 mM NaCl, 10 mM $MgCl_2$, pH 7.4. Temperature gradient 0.2°C/min. Absorbance measured at 254 nm.

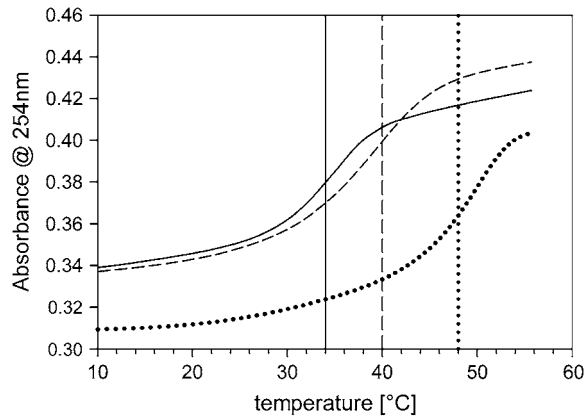

FIGURE 4 Melting curves recorded for [R_P-PS]-**1/2** (*dotted line*, $T_m = 51$°C); [Mix-PS]-**1/2** (*dash line*, $T_m = 40$°C); and [PO]-**1/2** (*solid line*, $T_m = 34$°C). Vertical lines indicate the observed corresponding melting temperature values. Temperature gradient 0.2°C/min. Buffer 10 mM Tris-HCl, 100 mM NaCl, 10 mM $MgCl_2$, pH 5.3. Absorbance measured at 254 nm.

observed. The above melting data indicate that phosphorothioate internucleotide linkages (especially those of R_P absolute configuration) substantially enhance thermal stability of parallel duplexes with 2′-OMe-RNA templates at neutrality, and the enhancement is also clearly observed for 2′-OH-RNA templates under acidic conditions.

Fluorescence quenching studies

Additional proof of the thermal stability and parallel orientation of strands was sought from fluorescence quenching studies. To that end, we synthesized three oligomers. The first was [R_P-PS]- BHQ_{PS}d(GAGGAAAGAGAG) (**6B**), which is an [R_P-PS]-**1** labeled at the 5′-end with a dark quencher acceptor (Black Hole Quencher, i.e., BHQ). The next two were 5′-FL-(2′-OMe)-CUCCUUUCUCUC (**4M**) and 5′-(2′-OMe)-CUCCUUUCUCUC-FL (**5M**), both being fluorescein (FL) labeled 2′-OMe-RNA oligomers complementary to **6B** according to Hoogsteen pairing.

When **4M** or **5M** were mixed with BHQ-labeled **6B**, they were expected to form the specific parallel complexes **VI** and **VII**, respectively (see Scheme 2). Because of the shorter distance between the BHQ and FL moieties in **VI** than in **VII**, stronger quenching of fluorescence should be observed. Simultaneously, fluorescence was measured for the corresponding triplex structures **4M/6B/3M** (**VIII**, Scheme 2) and **5M/6B/3M** (**IX**) to compare their stability with duplexes under investigation. The measurements revealed (Fig. 5) that, at r.t., the observed fluorescence intensity for **VI** was at least 10 times lower than that for **VII** (*solid* and *dotted lines*, respectively), indicating that BHQ and FL moieties are much closer in **VI** than in **VII**. This confirms the parallel orientation of the strands in the duplex. Moreover, these quenching efficiencies were virtually the same for the triplexes **VIII** and **IX** (*dash* and *dash-dot lines*, respectively). Thus, one can assume a remarkable similarity of overall geometry of the corresponding duplexes and triplexes. The same samples were used in a thermal dissociation experiment (Fig. 6). It must be pointed out that for a mixture of 5′-(2′-OMe)-CUCCUUUCUCUC-FL-3′ and 5′-(2′-OMe)-CUCUCUUUCCUC-3′ (**5M/3M**, no quencher present) the fluorescence intensity of the FL moiety significantly and steadily decreases with increasing temperature (Fig. 6, *triangles*). Nonetheless, we were able to observe remarkable increase of fluorescence for **VI** and **VII** above 55–60°C (*solid* and *dotted lines*, respectively), resulting from dissociation of the complexes around the melting point. This effect was smaller in the case of **VII,** where quenching was much less effective, so the fluorescence enhancement upon dissociation was smaller. Noteworthy, fluorescence in-

Scheme 2.

4M	5′-FL-CUCCUUUCUCUC	**5M**	5′-CUCCUUUCUCUC-FL
6B	5′-BHQ_{PS}GAGGAAAGAGAG	**6B**	5′-BHQ_{PS}GAGGAAAGAGAG
	VI		**VII**
4M	5′-FL-CUCCUUUCUCUC	**5M**	5′-CUCCUUUCUCUC-FL
6B	5′-BHQ_{PS}GAGGAAAGAGAG	**6B**	5′-BHQ_{PS}GAGGAAAGAGAG
3M	3′-CUCCUUUCUCUC	**3M**	3′-CUCCUUUCUCUC
	VIII		**IX**

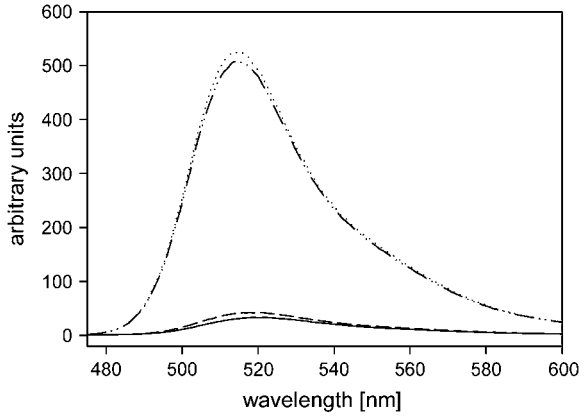

FIGURE 5 Fluorescence spectra for complexes **VI**, **VII**, **VIII**, and **IX** (*solid*, *dotted*, *dash*, and *dash-dot lines*, respectively). Parameters: r.t., excitation at 446 nm, excitation and emission slits 5 nm. Intensities given in arbitrary units.

tensities observed for both complexes **VI** and **VII** at 80°C are virtually identical and this indicates the presence of free, unassociated strands. Also, we observed only a slight increase of fluorescence for **VIII** above 55°C (*dashed line*), presumably resulting from partial dissociation of the complex below the melting point, confirming that thermal stability of triplexes is higher than that of corresponding parallel duplexes.

The oligomers **6B** and **4M** were also used in a titration experiment to establish stoichiometry of PS-DNA and RNA strands in the complex **VI**. A solution of **6B** (1 μM, 500 μL) was titrated with **4M** until final 1.8 μM concentration of the fluorescein-labeled RNA strand was reached (relative concentrations [FL-RNA]/[PS-BHQ-DNA] ranged from 0.2 to 1.8, a total volume of 50 μL was added). As a reference, the same aliquots of **4M** were added to a sample buffer and a

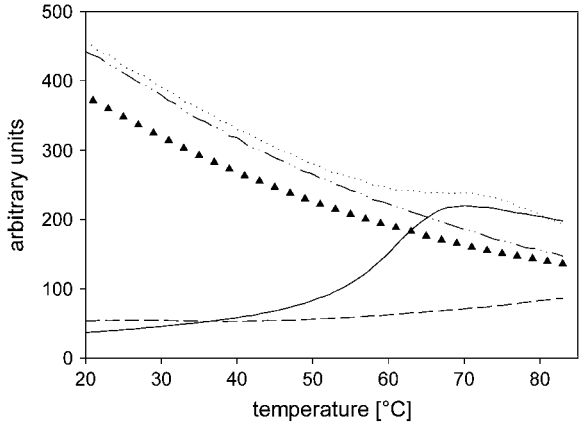

FIGURE 6 Fluorescence intensities at 516 nm for complexes **5M/3M** (*triangles*), **VI**, **VII**, **VIII**, and **IX** (*solid*, *dotted*, *dash*, and *dash-dot lines*, respectively) in melting experiment. Parameters: temperature gradient 1°C/min, data point collected with a 1°C increment, excitation at 446 nm, excitation and emission slits 5 nm. Intensities given in arbitrary units.

straight linear plot was obtained for fluorescence emission against RNA concentration (Supplementary Material, Fig. 3S, *open circles*; the data were corrected for a dilution factor). In the course of titration, at a relative concentration 1.1, a rapid increase of a slope for the second of two approximately linear segments of the corresponding plot (Supplementary Material. Fig. 3S, *open triangles*) was observed. It provides evidence that the association was almost complete at a stoichiometry 1:1, and the portions of **4M** added later have associated with the PS-BHQ-DNA strand to a very limited extent.

Possible mechanism of stabilization

Recently, in searching for a possible mechanism of stabilization of the RNA/[R_P-PS]-DNA/RNA triplex, we appreciated that the common structural feature of cytidine and uridine moieties is the presence of an oxygen in position 2 of the pyrimidine ring. Since also in these studies the R_P configuration of internucleotide phosphorothioate linkages in PS-DNA is required to stabilize the duplex efficiently, we suggest an analogous mechanism of stabilization, i.e., a water bridge between the pyrimidine O2 of the Hoogsteen strand and the anionic sulfur atom (Supplementary Material, Fig. 4S) whose ability to form strong charge-assisted hydrogen bonds has been discussed (35). Work on further kinetic, thermodynamic, and structural characterization of the structure, using fluorometry, NMR, FTIR, and osmometry techniques is in progress.

SUPPLEMENTARY MATERIAL

To view all of the supplemental files associated with this article, visit www.biophysj.org. Information available: A melting curve for a complex 5′-(2′-OMe)-r(CUCCUUUUUCUC)-3′/[R_P-PS]-d(GAGGAAAAAGAG)/3′-CUCCUUUUUCUC-5′ and a plot of dA/dT derivative; ORD CD spectra recorded during association experiment (85 → 8°C) with [PO]-dA_{12} and (2′-OMe)-U_{12} mixed at 1:2 molar ratio; and a plot for titration of [R_P-PS]- BHQ_{PS}d(GAGGAAAGAGAG) (**6B**) with 5′-FL-(2′-OMe)-CUCCUUUCUCUC (**4M**), a figure illustrating possible water bridge(s) between the phosphorothioate sulfur and uracil carbonyl oxygen in a parallel duplex [All-R_P-PS]-dA_2/U_2.

The authors thank Dr. Wojciech Stec for continuous interest and valuable discussions. Words of gratitude are directed to Dr. George M. Blackburn for critical reading of the manuscript and helpful suggestions.

This work was financially assisted by the State Committee for Scientific Research (Ministry of Science and Information, Poland, grant No. 3-T09A-072-26). The CD6 dichrograph has been financed by Polish Science Foundation BIMOL program.

REFERENCES

1. Watson, J. D., and F. H. Crick. 1953. Molecular structure of nucleic acids: a structure for deoxyribose nucleic acid. *Nature.* 171:737–738.
2. Felsenfeld, G., D. R. Davies, and A. Rich. 1957. Formation of a three-stranded polynucleotide molecule. *J. Am. Chem. Soc.* 79:2023–2024.
3. Mirkin, S. M., and M. D. Frank-Kamenetskii. 1994. H-DNA and related structures. *Annu. Rev. Biophys. Biomol. Struct.* 23:541–576.
4. Kang, C., X. Zhang, R. Ratliff, R. Moyzis, and A. Rich. 1992. Crystal structure of four-stranded *Oxytricha* telomeric DNA. *Nature.* 356:126–131.
5. Smith, F. W., and J. Feigon. 1992. Quadruplex structure of *Oxytricha* telomeric DNA oligonucleotides. *Nature.* 356:164–168.
6. Otto, C., G. A. Thomas, K. Rippe, T. M. Jovin, and W. L. Peticolas. 1991. The hydrogen-bonding structure in parallel-stranded duplex DNA is reverse Watson-Crick. *Biochemistry.* 30:3062–3069.
7. Lavelle, L., and J. R. Fresco. 1995. UV spectroscopic identification and thermodynamic analysis of protonated third strand deoxycytidine residues at neutrality in the triplex d(C^+-T)6:[d(A-G)6·d(C-T)6]; evidence for a proton switch. *Nucleic Acids Res.* 23:2692–2705.
8. Raghunathan, G., H. T. Miles, and V. Sasisekharan. 1994. Parallel nucleic acid helices with Hoogsteen base pairing: symmetry and structure. *Biopolymers.* 34:1573–1581.
9. Bhaumik, S. R., K. V. R. Chary, G. Govil, K. Liu, and H. T. Miles. 1998. A novel palindromic triple-stranded structure formed by homopyrimidine dodecamer d-CTTCTCCTCTTC and homopurine hexamer d-GAAGAG. *Nucleic Acids Res.* 26:2981–2988.
10. Tchurikov, N. A., B. K. Chernov, Y. B. Golova, and Y. D. Nechipurenko. 1989. Parallel DNA: generation of a duplex between two *Drosophila* sequences in vitro. *FEBS Lett.* 257:415–418.
11. Tchurikov, N. A., A. K. Shchyolkina, O. F. Borissova, and B. K. Chernov. 1992. Southern molecular hybridization experiments with parallel complementary DNA probes. *FEBS Lett.* 297:233–236.
12. Borisova, O. F., A. K. Shchyolkina, B. K. Chernov, and N. A. Tchurikov. 1993. Relative stability of AT and GC pairs in parallel DNA duplex formed by a natural sequence. *FEBS Lett.* 322:304–306.
13. Tchurikov, N. A., L. G. Chistyakova, G. B. Zavilgelsky, I. V. Manukhov, B. K. Chernov, and Y. B. Golova. 2000. Gene-specific silencing by expression of parallel complementary RNA in *Escherichia coli*. *J. Biol. Chem.* 275:26523–26529.
14. Westhof, E., and M. Sundaralingam. 1980. X-ray structure of a cytidylyl-3′,5′-adenosine-proflavine complex: a self-paired parallel-chain double helical dimer with an intercalated acridine dye. *Proc. Natl. Acad. Sci. USA.* 77:1852–1856.
15. Hakoshima, T., T. Fukui, M. Ikehara, and K. Tomita. 1981. Molecular structure of a double helix that has non-Watson-Crick type base pairing formed by 2-substituted poly(A) and poly(U). *Proc. Natl. Acad. Sci. USA.* 78:7309–7313.
16. Pattabiraman, N. 1986. Can the double helix be parallel? *Biopolymers.* 25:1603–1606.
17. Mohammadi, S., R. Klement, A. K. Shchyolkina, J. Liquier, T. M. Jovin, and E. Taillandier. 1998. FTIR and UV spectroscopy of parallel-stranded DNAs with mixed A-T/G-C sequences and their A-T/I-C analogues. *Biochemistry.* 37:16529–16537.
18. Zhou, N., M. W. Germann, J. H. van de Sande, N. Pattabiraman, and H. J. Vogel. 1993. Solution structure of the parallel-stranded hairpin d(T8 C4A8) as determined by two-dimensional NMR. *Biochemistry.* 32:646–656.
19. Bhaumik, S. R., K. V. R. Chary, G. Govil, K. Liu, and H. T. Miles. 2002. NMR structure of a parallel-stranded DNA duplex at atomic resolution. *Nucleic Acids Res.* 30:1500–1511.
20. Cubero, E., A. Aviñó, B. G. de la Torre, M. Frieden, R. Eritja, F. J. Luque, C. González, and M. Orozco. 2002. Hoogsteen-based parallel-stranded duplexes of DNA. Effect of 8-amino-purine derivatives. *J. Am. Chem. Soc.* 124:3133–3142.
21. Kandimalla, E. R., and S. Agrawal. 1996. Hoogsteen DNA duplexes of 3′-3′- and 5′-5′-linked oligonucleotides and triplex formation with RNA and DNA pyrimidine single strands: experimental and molecular modeling studies. *Biochemistry.* 35:15332–15339.
22. van de Sande, J. H., N. B. Ramsing, M. W. Germann, W. Elhorst, B. W. Kalisch, E. von Kitzing, R. T. Pon, R. C. Clegg, and T. M. Jovin. 1988. Parallel stranded DNA. *Science.* 241:551–557.

23. Rajeev, K. G., V. R. Jadhav, and K. N. Ganesh. 1997. Triplex formation at physiological pH: comparative studies on DNA triplexes containing 5-Me-dC tethered at N4 with spermine and tetraethyleneoxyamine. *Nucleic Acids Res.* 25:4187–4193.

24. Roig, V., and U. Asseline. 2003. Oligo-2′-deoxyribonucleotides containing uracil modified at the 5-position with linkers ending with guanidinium groups. *J. Am. Chem. Soc.* 125:4416–4417.

25. Verma, S., and F. Eckstein. 1998. Modified oligonucleotides: synthesis and strategy for users. *Annu. Rev. Biochem.* 67:99–134.

26. Dagle, J. M., J. L. Littig, L. B. Sutherland, and D. L. Weeks. 2000. Targeted elimination of zygotic messages in *Xenopus laevis* embryos by modified oligonucleotides possessing terminal cationic linkages. *Nucleic Acids Res.* 28:2153–2157.

27. Nielsen, P. E., and M. Egholm. 1999. An introduction to peptide nucleic acid. *Curr. Issues Mol. Biol.* 1:89–104.

28. Summerton, J. 1999. Morpholino antisense oligomers: the case for an RNase H-independent structural type. *Biochim. Biophys. Acta.* 1489: 141–158.

29. Stec, W. J., and A. Wilk. 1994. Stereocontrolled synthesis of oligo (nucleoside phosphorothioate)s. *Angew. Chem. Int. Ed. Engl.* 33:709–722.

30. Wilk, A., and W. J. Stec. 1995. Analysis of oligo(deoxynucleoside phosphorothioate)s and their diastereomeric composition. *Nucleic Acids Res.* 23:530–534.

31. Stec, W. J., B. Karwowski, M. Boczkowska, P. Guga, M. Koziołkiewicz, M. Sochacki, M. Wieczorek, and J. Błaszczyk. 1998. Deoxyribonucleoside 3′-O-(2-thio- and 3′-O-(2-oxo-''spiro''-4.4-pentamethylene-1.3.2-oxathiaphospholanes): monomers for stereocontrolled synthesis of oligo(nucleoside phosphorothioate)s and chimeric PS/PO oligonucleotides. *J. Am. Chem. Soc.* 120:7156–7167.

32. Guga, P., and W. J. Stec. 2003. Current Protocols in Nucleic Acid Chemistry. S. L. Beaucage, D. E. Bergstrom, G. D. Glick, and R. A. Jones, editors. John Wiley and Sons, Hoboken, NJ.

33. Boczkowska, M., P. Guga, and W. J. Stec. 2002. Stereodefined phosphorothioate analogues of DNA: relative thermodynamic stability of the model PS-DNA/DNA and PS-DNA/RNA complexes. *Biochemistry.* 41:12483–12487.

34. Freier, S. M., and K. H. Altmann. 1997. The ups and downs of nucleic acid duplex stability: structure-stability studies on chemically modified DNA:RNA duplexes. *Nucleic Acids Res.* 25:4429–4443.

35. Guga, P., M. Boczkowska, M. Janicka, A. Maciaszek, S. Kuberski, and W. J. Stec. 2007. Unusual thermal stability of RNA/[Rp-PS]-DNA/RNA triplexes containing a homopurine DNA strand. *Biophys. J.* 92: 2507–2515.

36. Brown, T., C. E. Pritchard, G. Turner, and S. A. Salisbury. 1989. A new base-stable linker for solid-phase oligonucleotide synthesis. *J. Chem. Soc. Chem. Commun.*891–893.

37. Brown, T., and D. J. S. Brown. 1991. Modern machine-aided methods of oligodeoxyribonucleotide synthesis. *In* Oligonucleotides and Analogues: A Practical Approach. F. Eckstein, editor. IRL Press, Oxford, UK.

38. González, C., W. Stec, A. Kobylańska, R. I. Hogrefe, M. Reynolds, and T. L. James. 1994. Structural study of a DNA·RNA hybrid duplex with a chiral phosphorothioate moiety by NMR: extraction of distance and torsion angle constraints and imino proton exchange rates. *Biochemistry.* 33:11062–11072.

39. González, C., W. J. Stec, M. A. Reynolds, and T. L. James. 1995. Structure and dynamics of a DNA·RNA hybrid duplex with a chiral phosphorothioate moiety: NMR and molecular dynamics with conventional and time-averaged restraints. *Biochemistry.* 34:4969–4982.

40. Bachelin, M., G. Hessler, G. Kurz, J. G. Hacia, P. B. Dervan, and H. Kessler. 1998. Structure of a stereoregular phosphorothioate DNA/RNA duplex. *Nat. Struct. Biol.* 5:271–276.

41. Furrer, P., T. M. Billeci, A. Donati, C. Kojima, B. Karwowski, A. Sierzchała, W. J. Stec, and T. L. James. 1999. Structural effect of complete [Rp]-phosphorothioate and phosphorodithioate substitutions in the DNA strand of a model antisense inhibitor-target RNA complex. *J. Mol. Biol.* 285:1609–1622.

42. Kanaori, K., Y. Tamura, T. Wada, M. Nishi, H. Kanehara, T. Morii, K. Tajima, and K. Makino. 1999. Structure and stability of the consecutive stereoregulated chiral phosphorothioate DNA duplex. *Biochemistry.* 38:16058–16066.